Figure S1

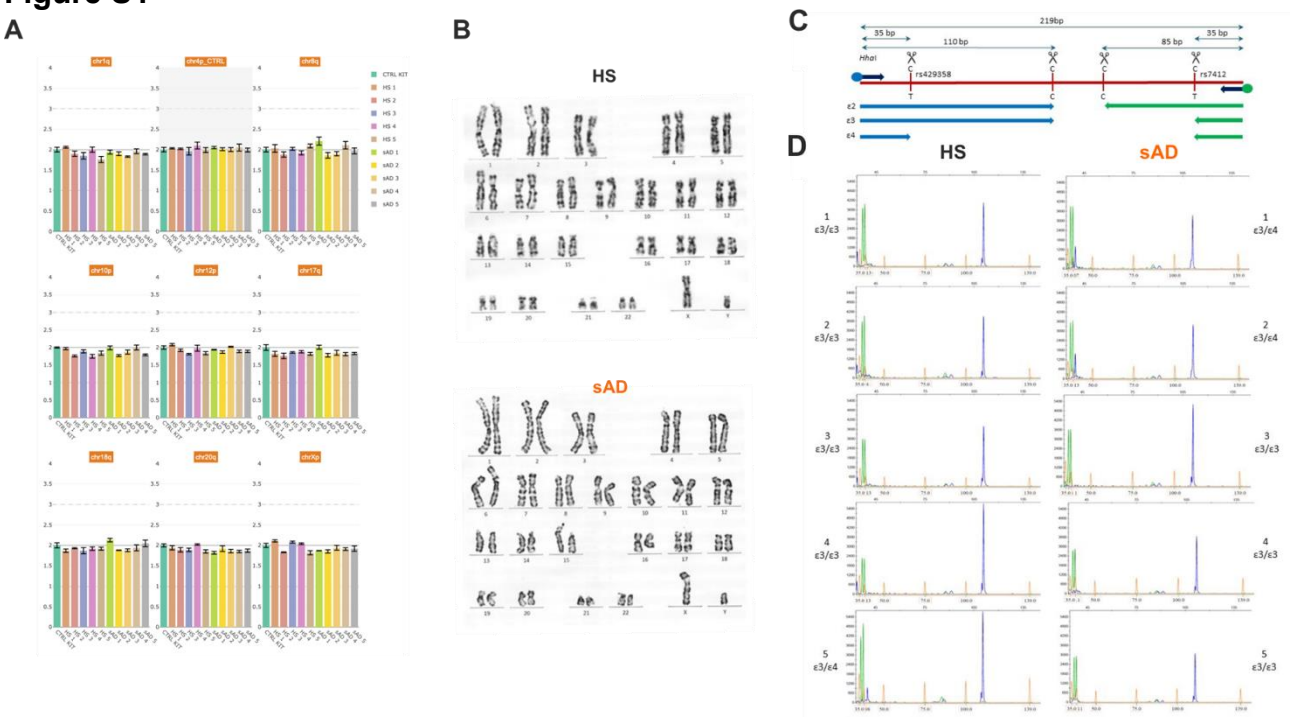

Fig. S1. q-PCR genetic analysis to detect small chromosome abnormalities in hiPSC lines. (A) The copy numbers of chr1q, chr8q, chr10p, chr12p, chr17q, chr18q, chr20q and chrXp were normalized to chr4p expression which was set to be 2. (n=5 HSI, n=5 sAD). (B) Boxes indicate a karyotype analysis of HS (left) and sAD (right). Both karyotype are 46,XY and no showing genetic aberration. (C) The figure shows the amplification of the exon 4 of APOE. The PCR was performed using both fluorophore-marked primers flanking the rs429358 and rs7412 SNPs. This region (219 bp) has four HhaI restriction sites (GCG^C) that allow to obtain different length fragments corresponding to the ε2, -3 or -4 alleles (blue and green arrows). For genotyping, the size of the fragments are: 85-110bp for ε2-/ε2; 35-110bp for ε3/ε3 and both at 35bp for ε4/ ε4. In (D) are shown the genotype of the HS (left) and sAD (right) cell cultures.

Figure S2

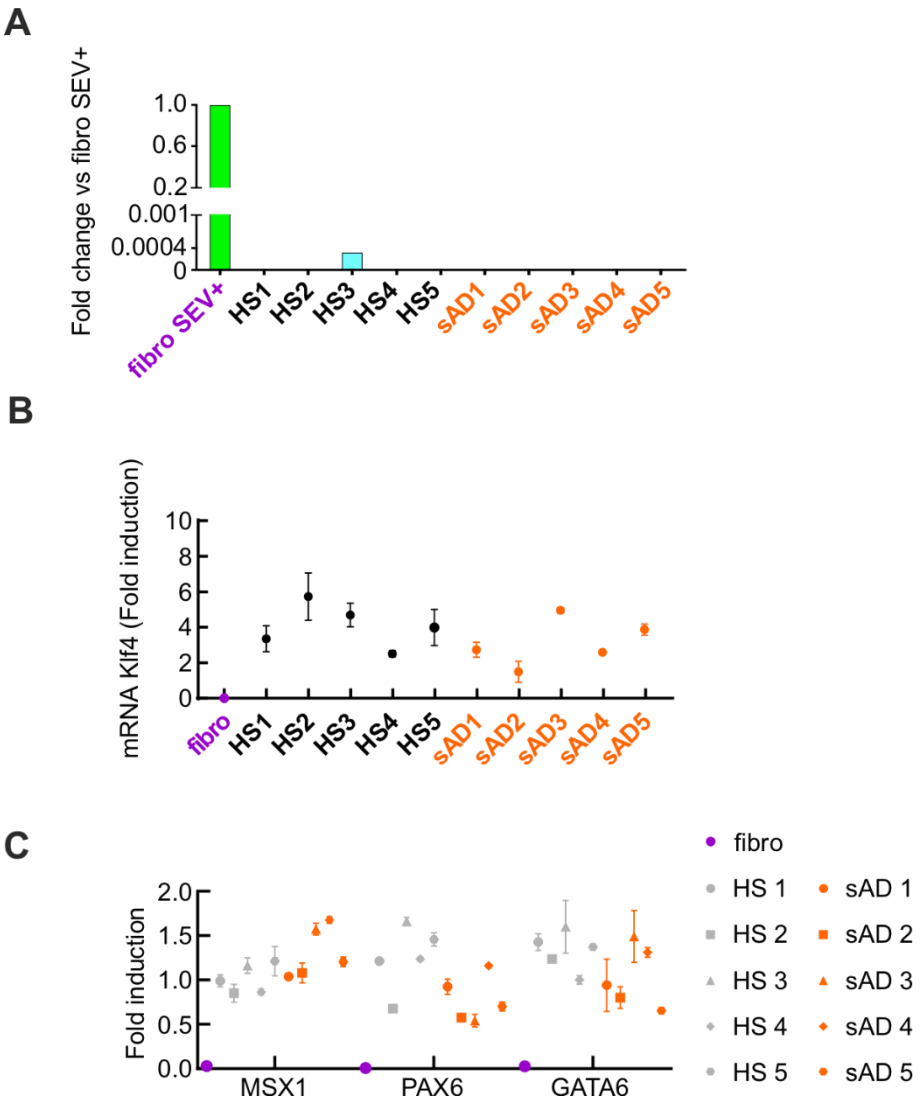

Fig. S2. Verification of Sendai virus clearance and differentiation potential of hiPSCs derived from HS and sAD patients. (A) RT-PCR analysis confirms the successful elimination of the Sendai virus from hiPSCs derived from HS and sAD patients. Infected fibroblasts were used as positive controls 5 days after SeV transduction.. (**B**) mRNA expression levels of Klf4 to futher validate the pluripotency. Human skin fibroblasts were used as negative controls for pluripotency. **(**hiPSCs (**C**) qPCR for mRNA expression of three germ layer genes. Quantification of expression of the ectoderm (PAX6), mesoderm (MSX1), and endoderm (GATA6) markers compared to hiPSCs. Matched hiPSCs, from which the differentiated germ layer was derived, were utilized as negative controls.

Figure S3

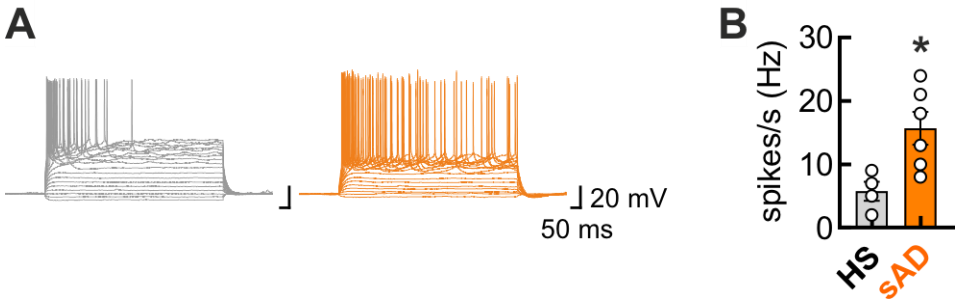

Fig. S3. Action potential firing properties in neurons derived from HS and sAD patients. (A) Representative traces showing current-evoked firing of HS-hNs (grey) and sAD-hNs (orange). (B) Bar graph depicting quantification of evoked firing in the experimental conditions shown in (E) (n= 4 HS, n=6 sAD). Data are expressed as mean ± SEM. **P < 0.05; statistics by two-tailed Student's t test.

Figure S4

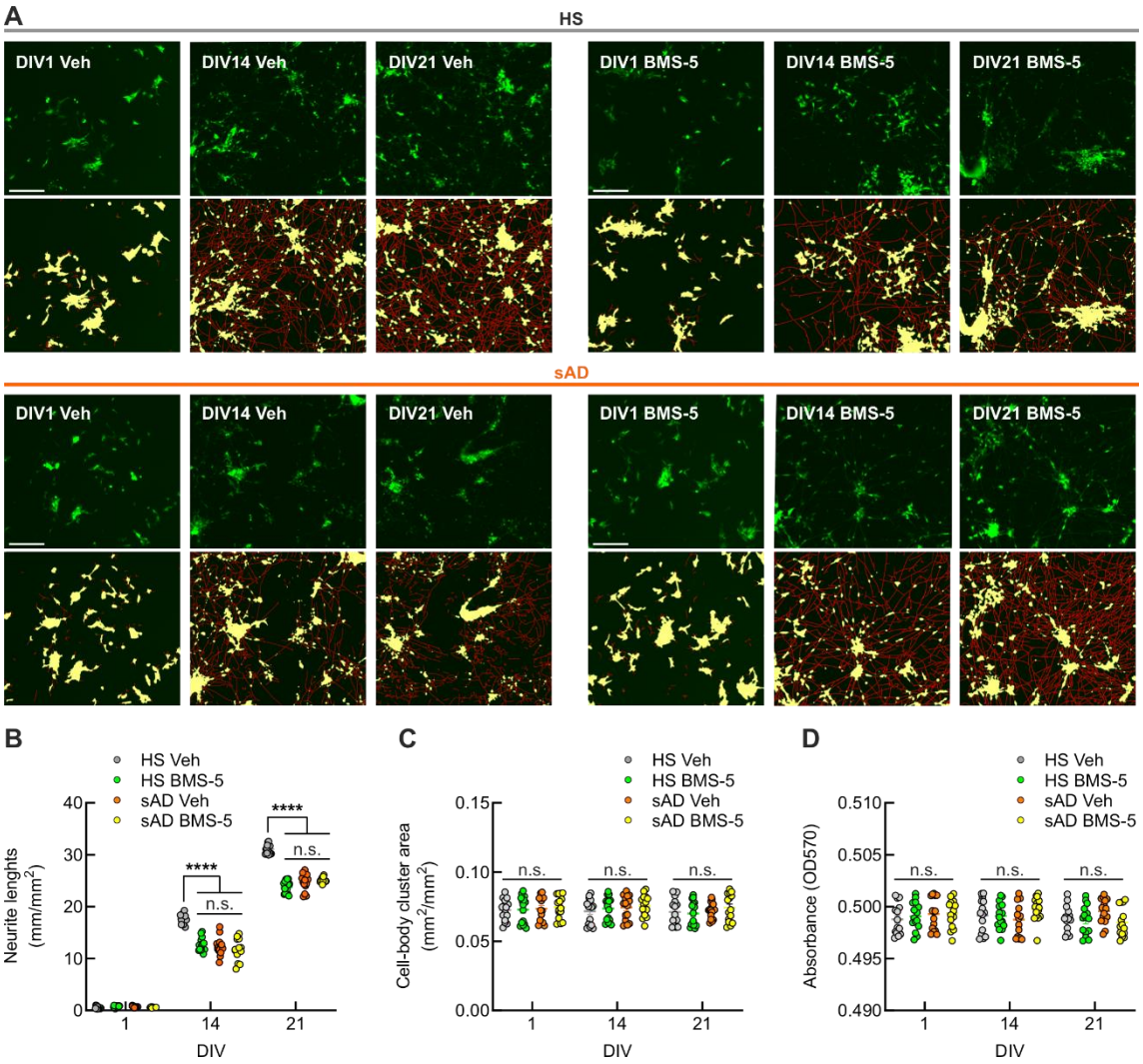

Fig. S4. Effect of BMS-5 treatment on neuronal morphology and neurite outgrowth in neurons derived from HS and sAD patients at different time points. (A) Representative images showing neuronal morphology over time under vehicle (Veh) or BMS-5 treatment in HS and sAD neurons. EGFP (green) labels neuronal processes, while yellow and red indicate neurite tracing and soma, respectively. Neurons were analyzed at DIV1, DIV14, and DIV21 (B) Neurite length appears reduced in HS BMS-5 hNS, sAD Veh hNs, sAD BMS-5 hNs compared to HS Veh hNs at DIV14 and DIV21. At DIV14, neurite length decreased by 28.0% in sAD Veh ($p<0.0001$), 30.4% in HS BMS-5 ($p<0.0001$), and 33.7% in sAD BMS-5 ($p<0.0001$) compared to HS Veh. At DIV21, neurite length was reduced by 23.6% in sAD Veh ($p<0.0001$) and 19.4% in sAD BMS-5 ($p<0.0001$) relative to HS Veh. (C) No significant changes in cell body clusters or cell viability were observed in each hNs condition at DIV1, DIV14 and DIV21. (D) No significant changes in cell viability were observed in each hNs condition at DIV1, DIV14 and DIV21. Scale bars: 50 µm. Each dot in Figs B-D represents a triplicate of an experiment conducted on n = 5/group. Data are presented as mean ± SEM, n.s. $p > 0.05$, **** **$p < 0.0001$,** assessed by 2way ANOVA-Sidak's multiple comparisons.

Uncropped images of Fig.2

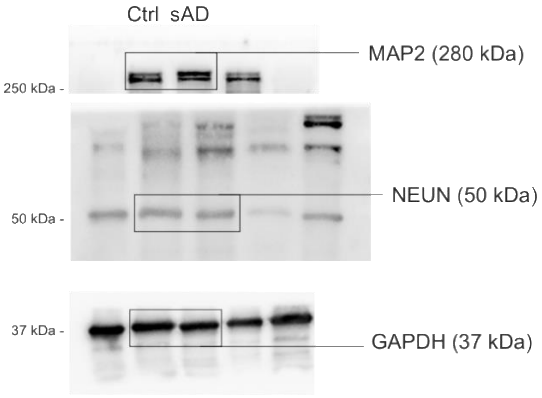

Uncropped images of Fig. 3

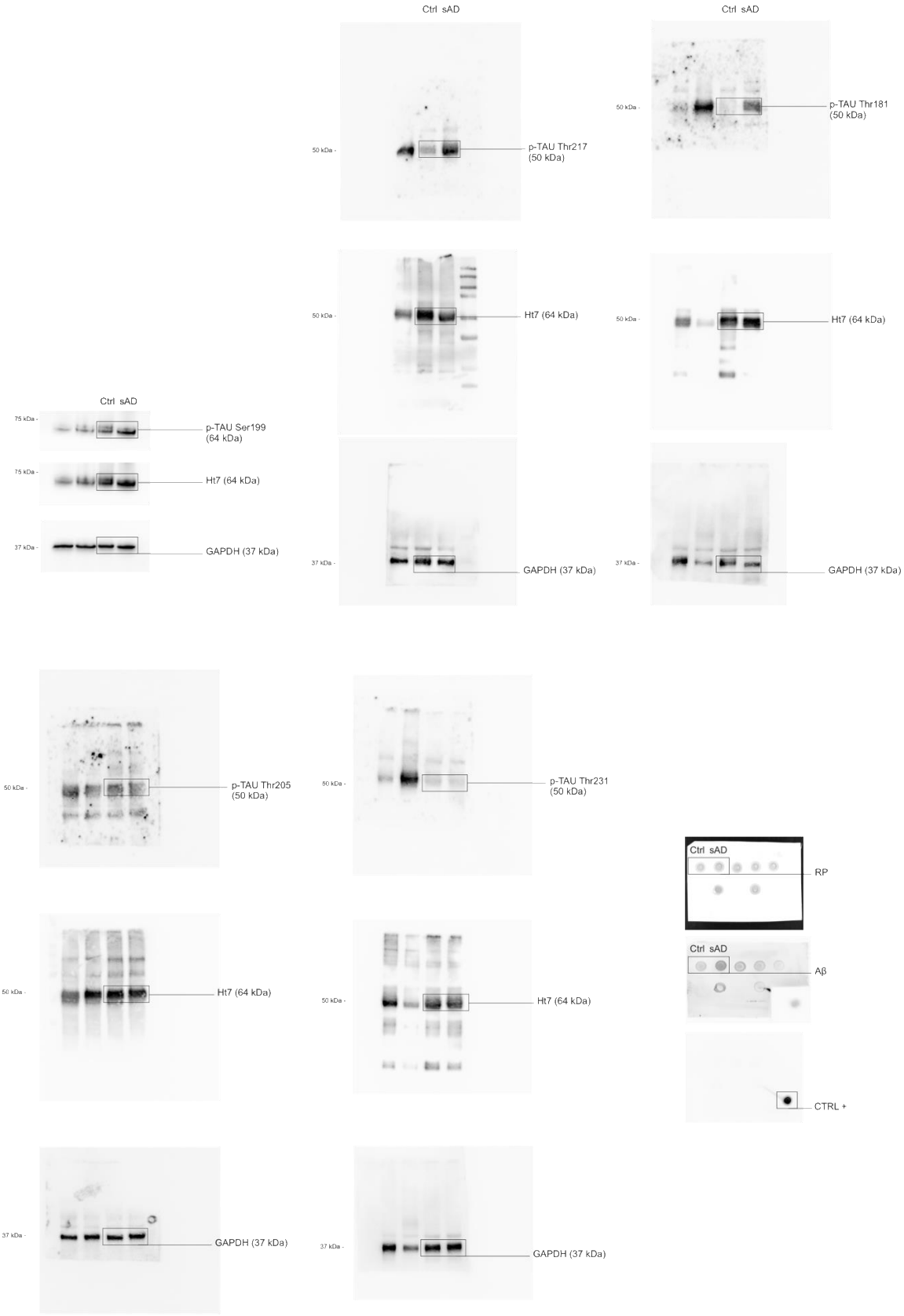

Uncropped images of Fig.6

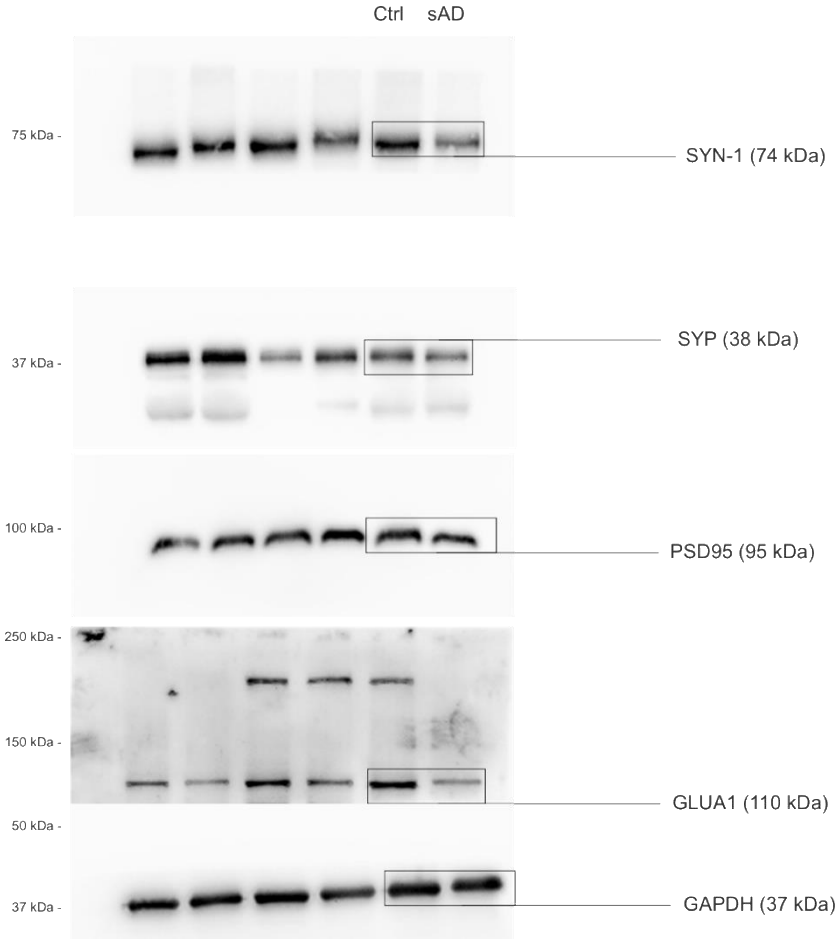

Uncropped images of Fig.7